# Formación de Imágenes en el Microscopio Electrónico de Transmisión

MT774

Caracterización de Materiales

Alejandro Zúñiga

12 de septiembre de 2007

# Contraste

Contraste (C) se define en términos de la diferencia en intensidad (ΔI) entre dos áreas adyacentes de una imagen

$$C = \frac{(I_2 - I_1)}{I_1} = \frac{\Delta I}{I_1}$$

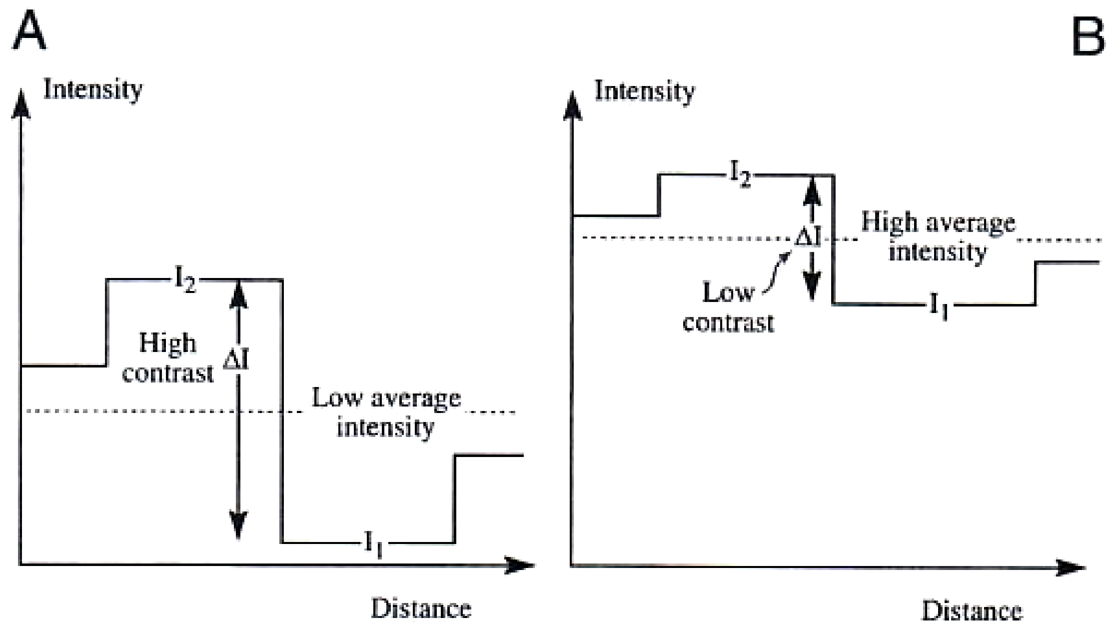


**Figure 22.1.** Schematic intensity profiles across an image showing (A) different intensity levels ($I_1$ and $I_2$) and the difference ($\Delta I$) between them, which defines the contrast. Generally, in a TEM, if the overall intensity is increased (B) the contrast decreases.

# Tipos de contraste

- Contraste por masa-espesor
- Contraste por difracción
- Contraste por fase
- Contraste Z

# Contraste por masa-espesor

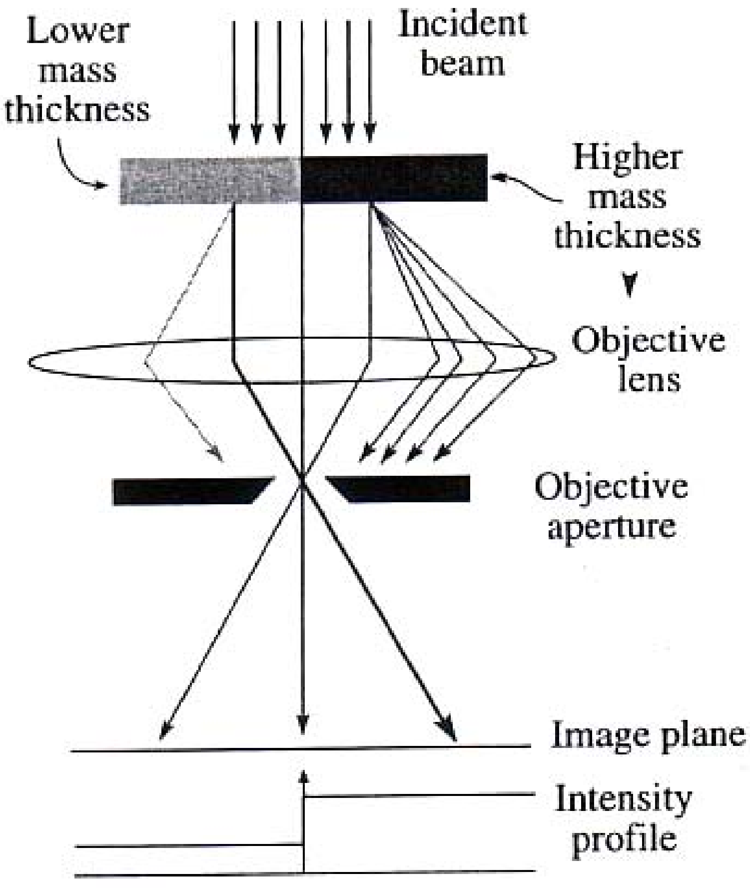


**Figure 22.4.** Mechanism of mass-thickness contrast in a BF image. Thicker or higher-Z areas of the specimen (darker) will scatter more electrons off axis than thinner or lower-mass (lighter) areas. Thus fewer electrons from the darker region fall on the equivalent area of the image plane (and subsequently the screen), which therefore appears darker in BF images.

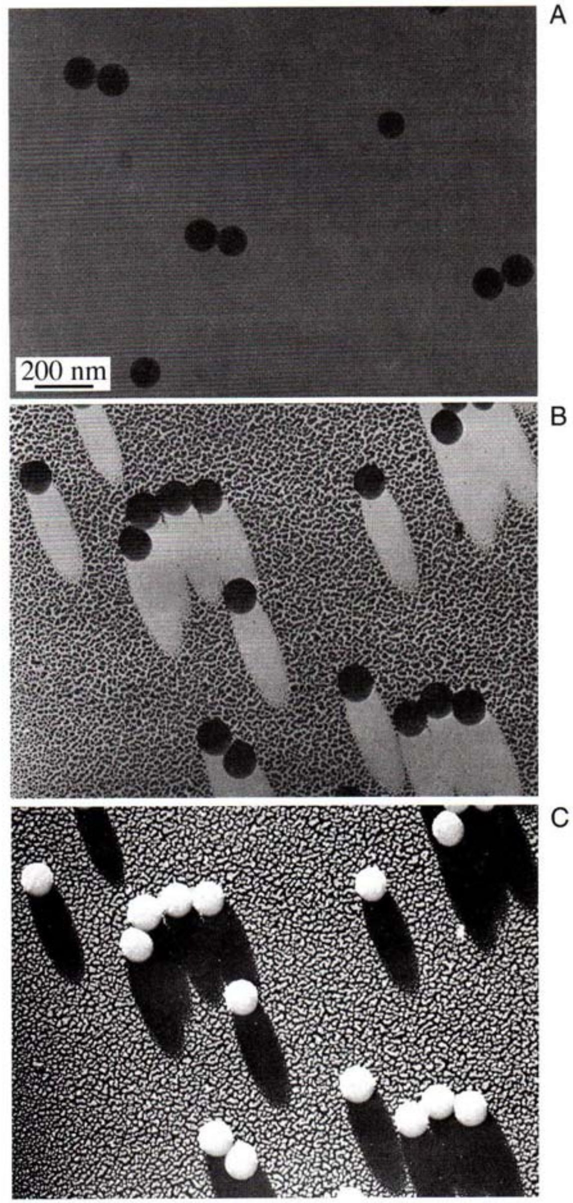


**Figure 22.5.** (A) TEM BF image of latex particles on a carbon support film showing thickness contrast only. (B) Latex particles on a carbon film shadowed to reveal the shape of the particles through the addition of selective mass contrast to the image. (C) Reverse print of (B) exhibits a 3D appearance.

# Contraste por difracción

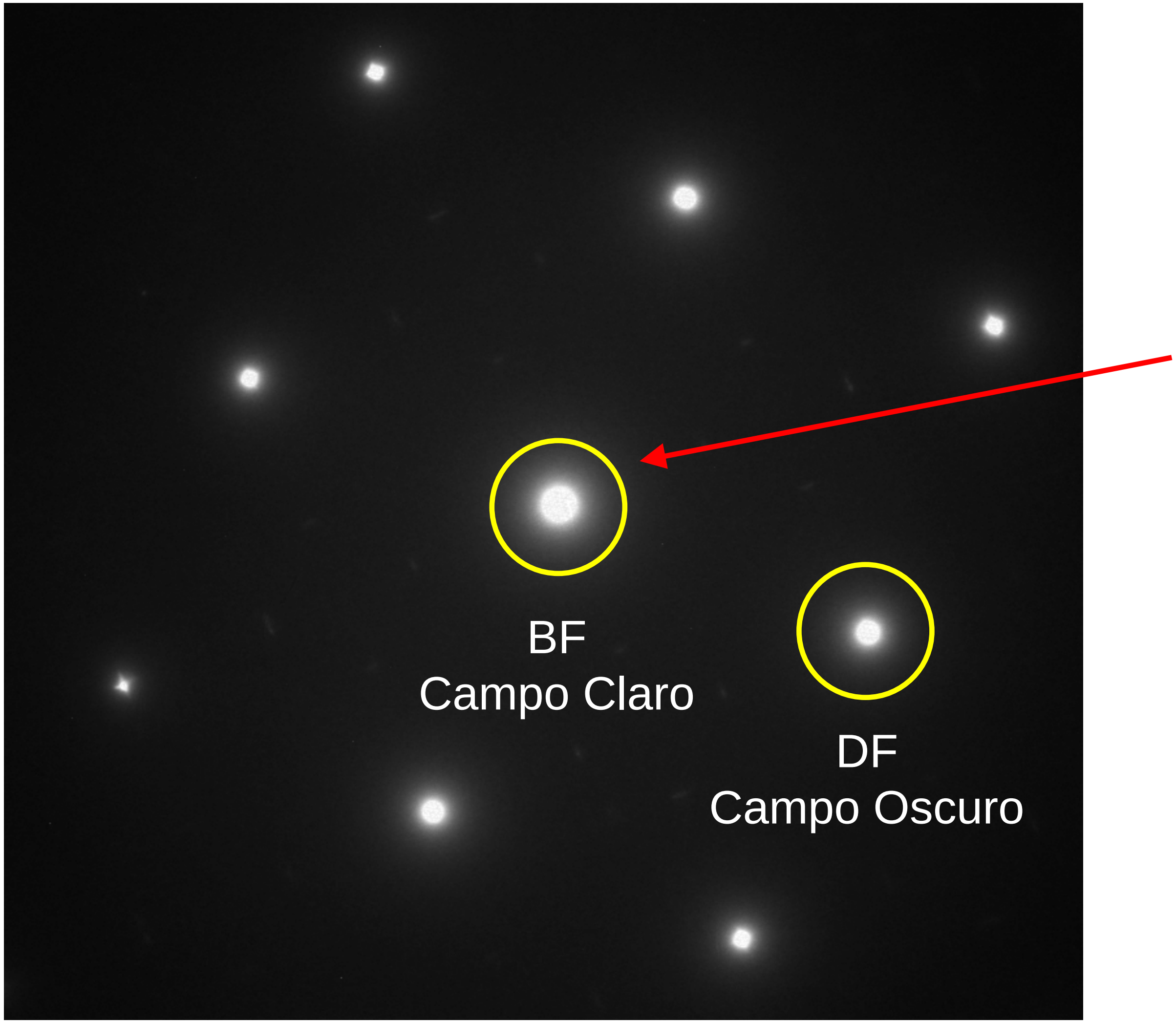


Apertura
en el plano
focal del
lente objetivo

# Imágenes – Contraste por difracción

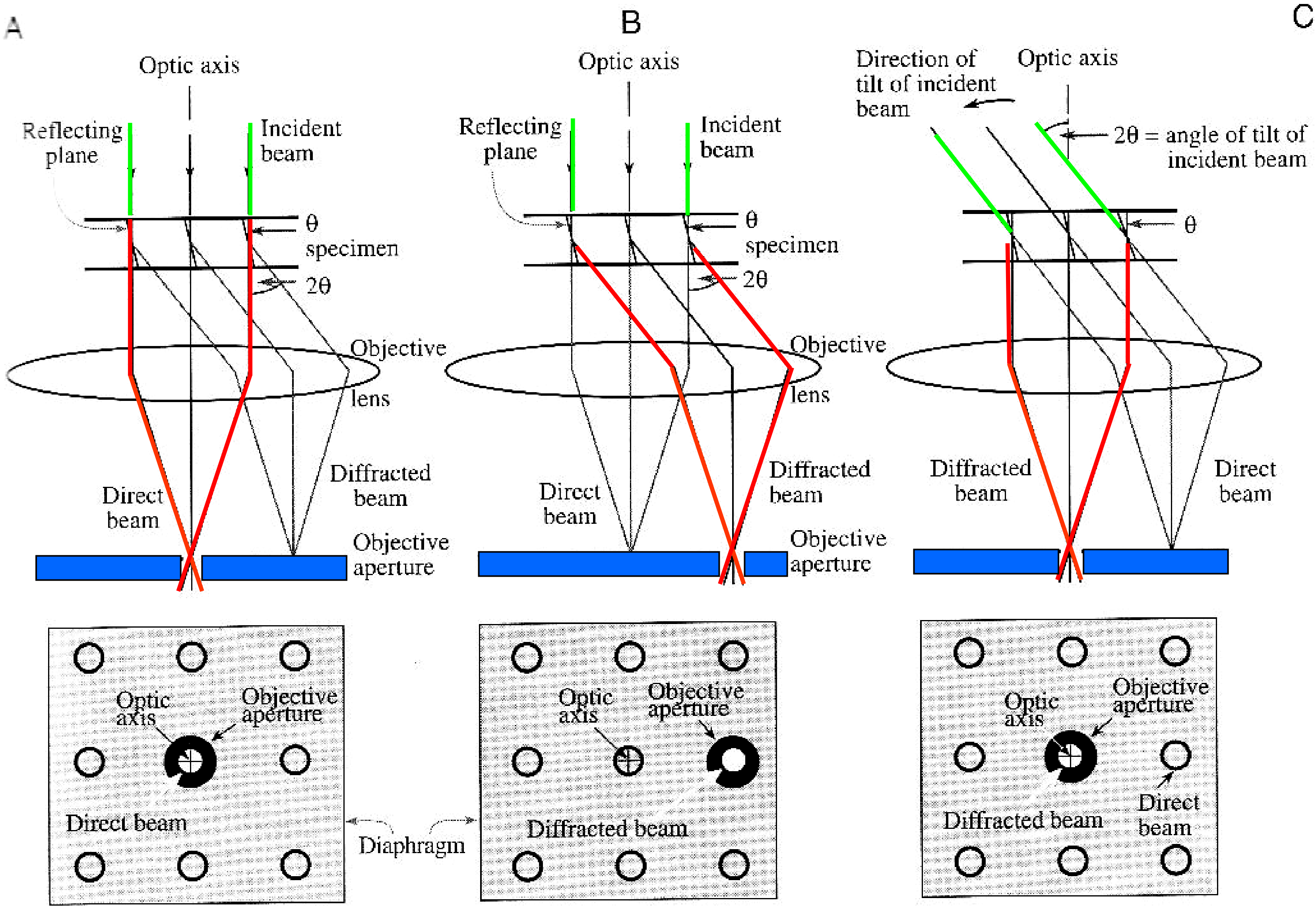


**Campo Claro (BF)** **Campo Oscuro (DF)**

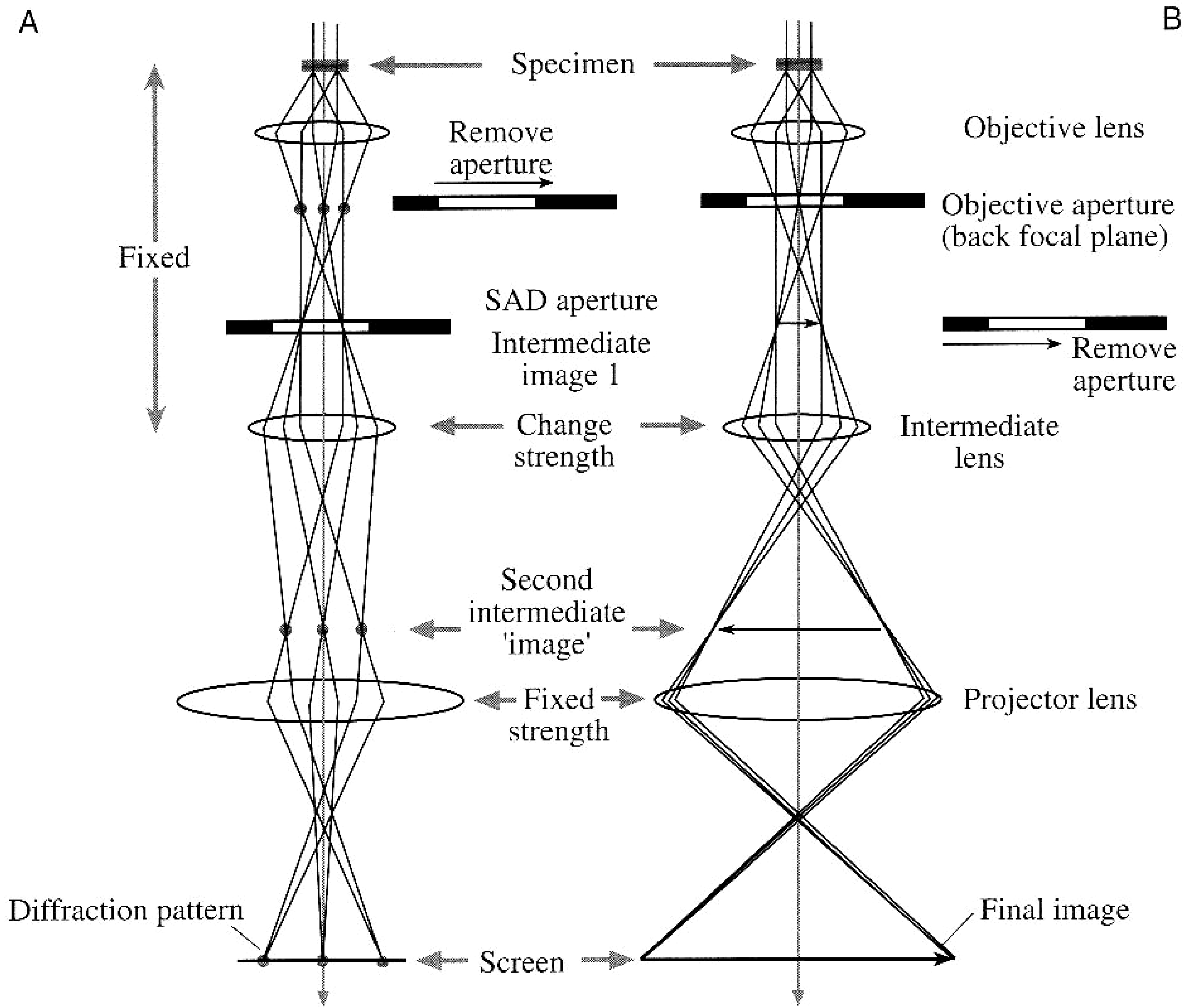


**Figure 9.12.** The two basic operations of the TEM imaging system involve (A) projecting the diffraction pattern on the viewing screen and (B) projecting the image onto the screen. In each case the intermediate lens selects either the back focal plane or the image plane of the objective lens as its object.

# Ejemplos - Contraste por difracción

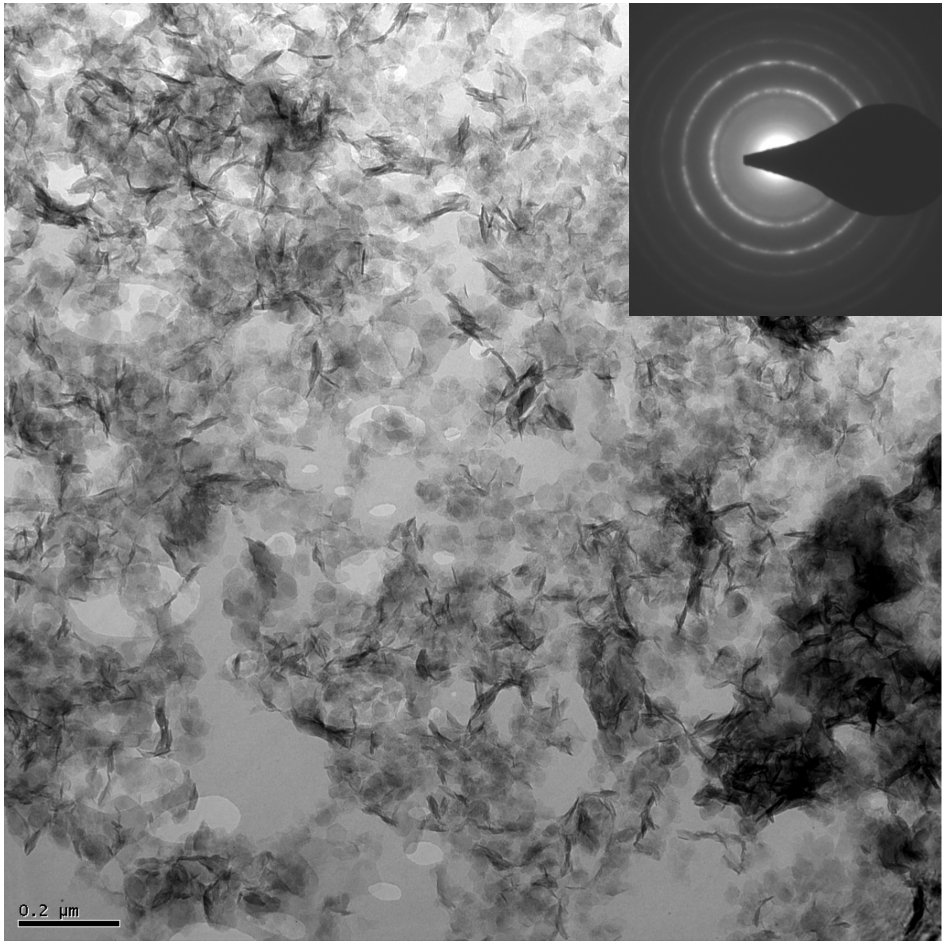


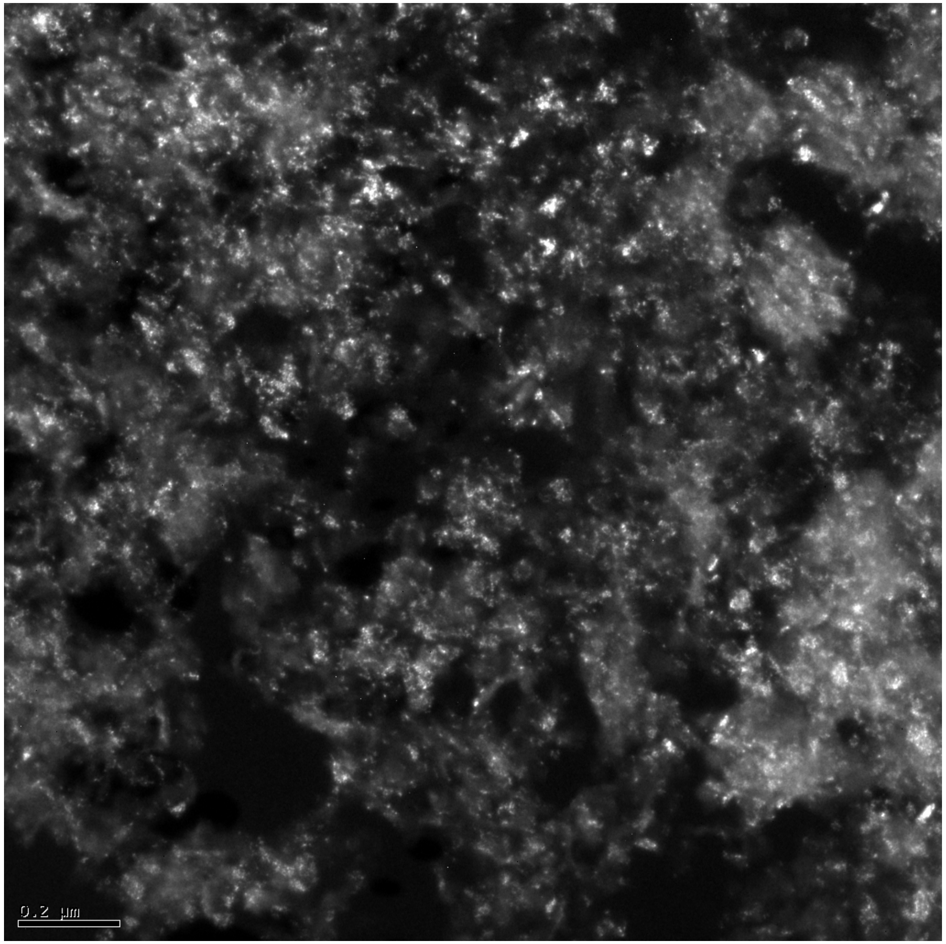


Campo Claro

Campo Oscuro

**Hidrotalcita policristalina** $\left[Mg_{1-x}\,Al_x(OH)_2\right]A^{n-}_{x/n}\cdot m\,H_2O$

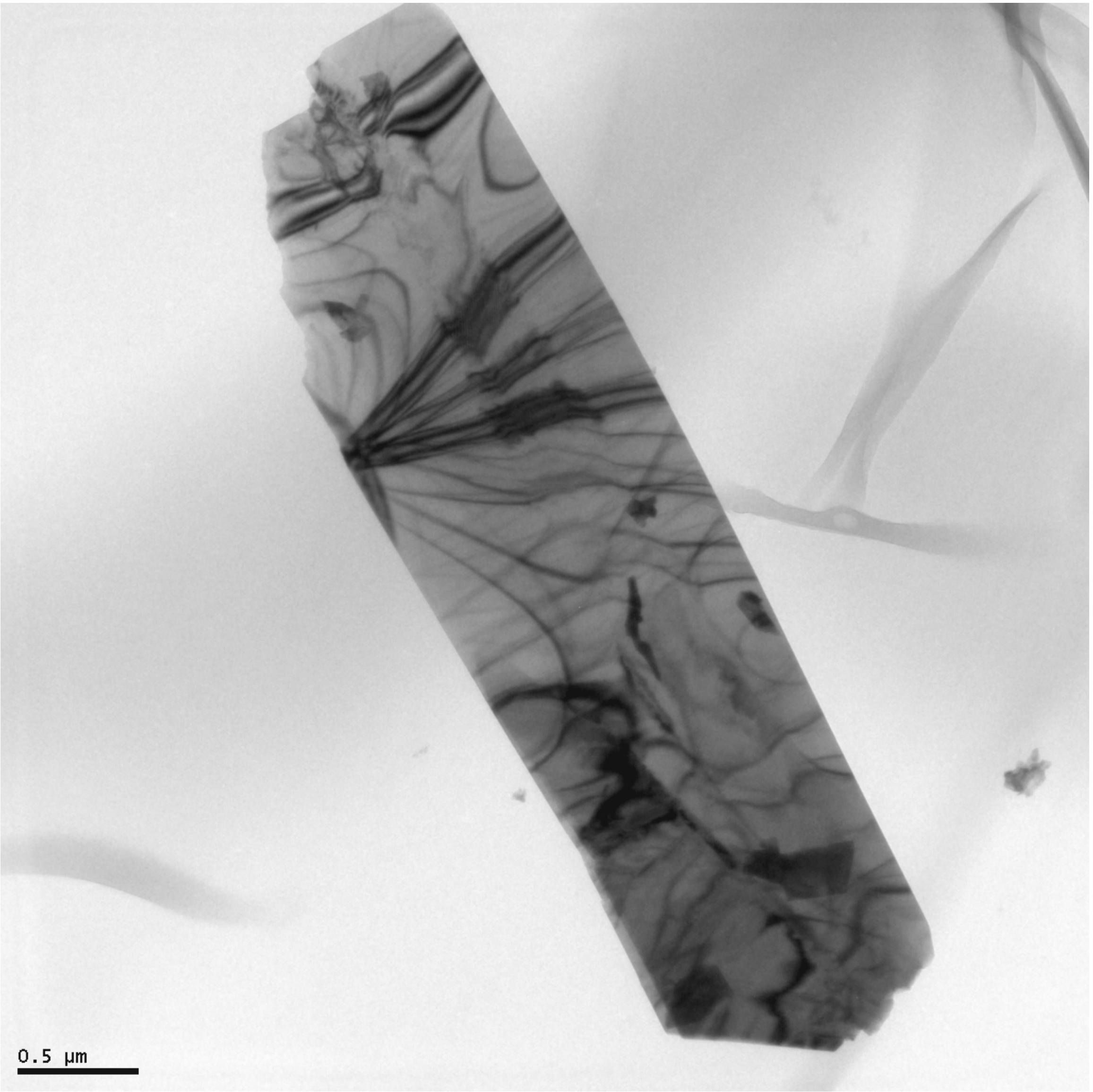


Campo Claro

**Nanoplacas de CuO**

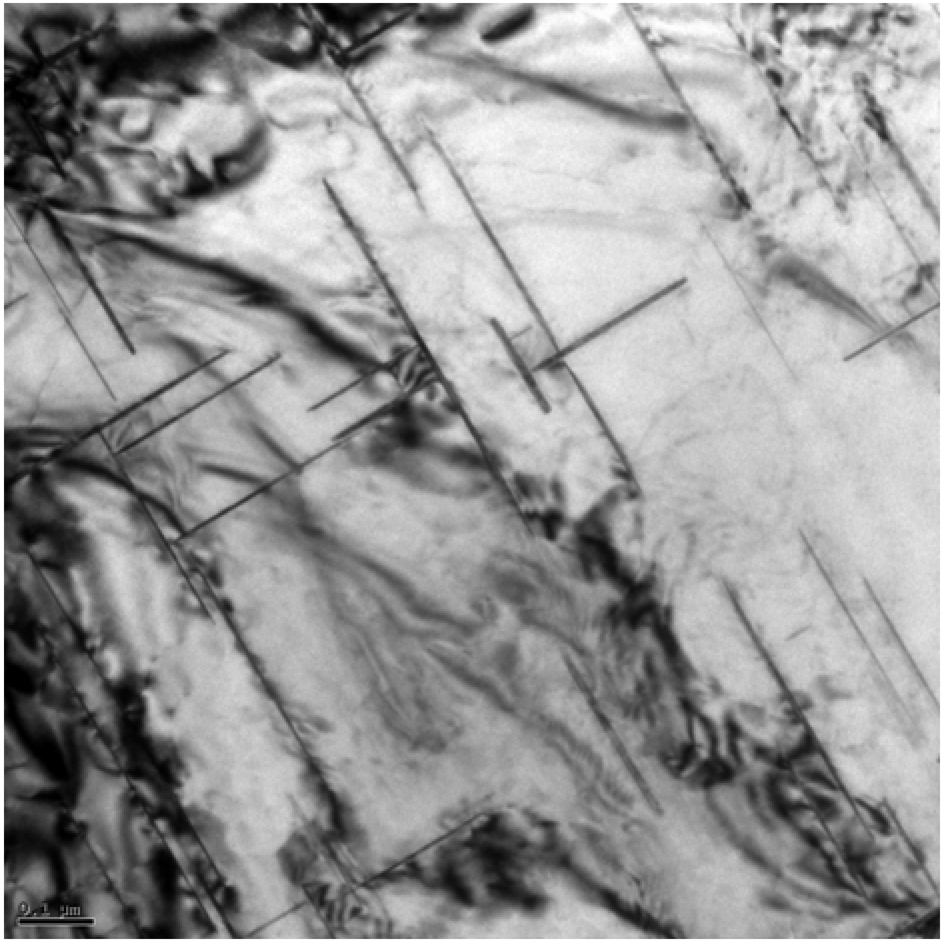


Campo Claro

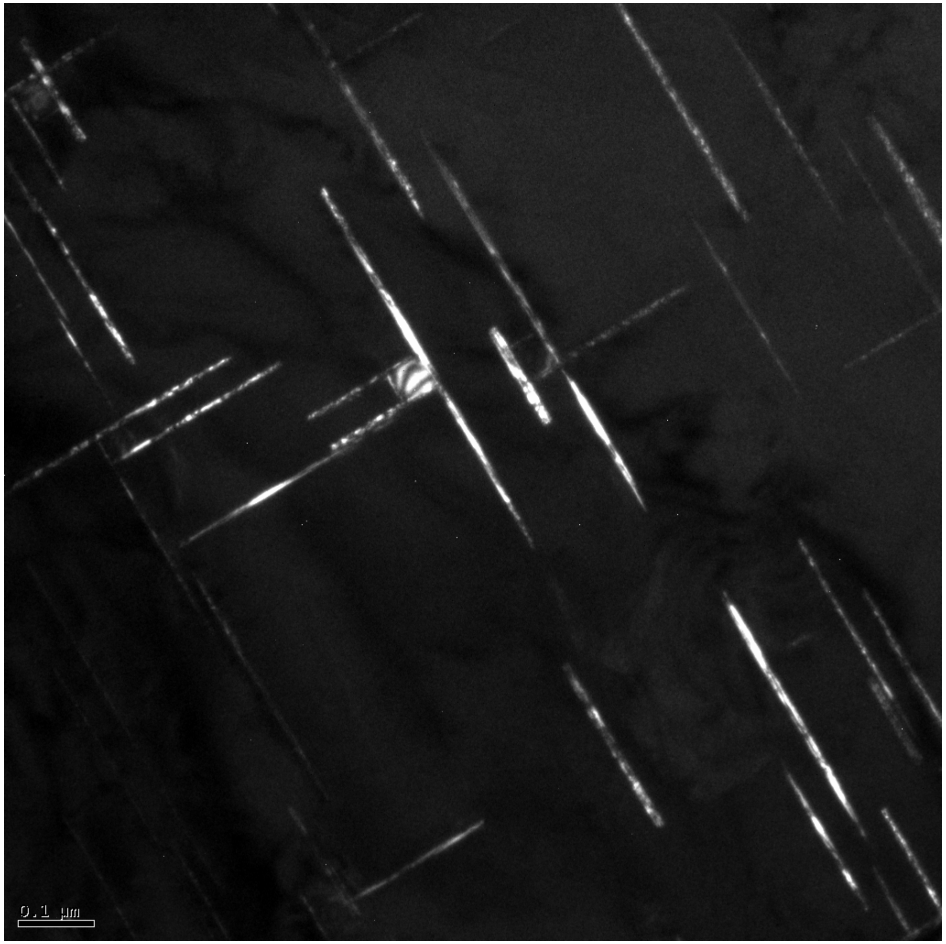


Campo Oscuro

**Al-Cu Envejecido**

# Líneas de espesor

$$\left|\phi_{\mathbf{g}}\right|^2 = \left(\frac{\pi t}{\xi_{\mathbf{g}}}\right)^2 \frac{\sin^2(\pi t s_{\mathrm{eff}})}{(\pi t s_{\mathrm{eff}})^2}$$

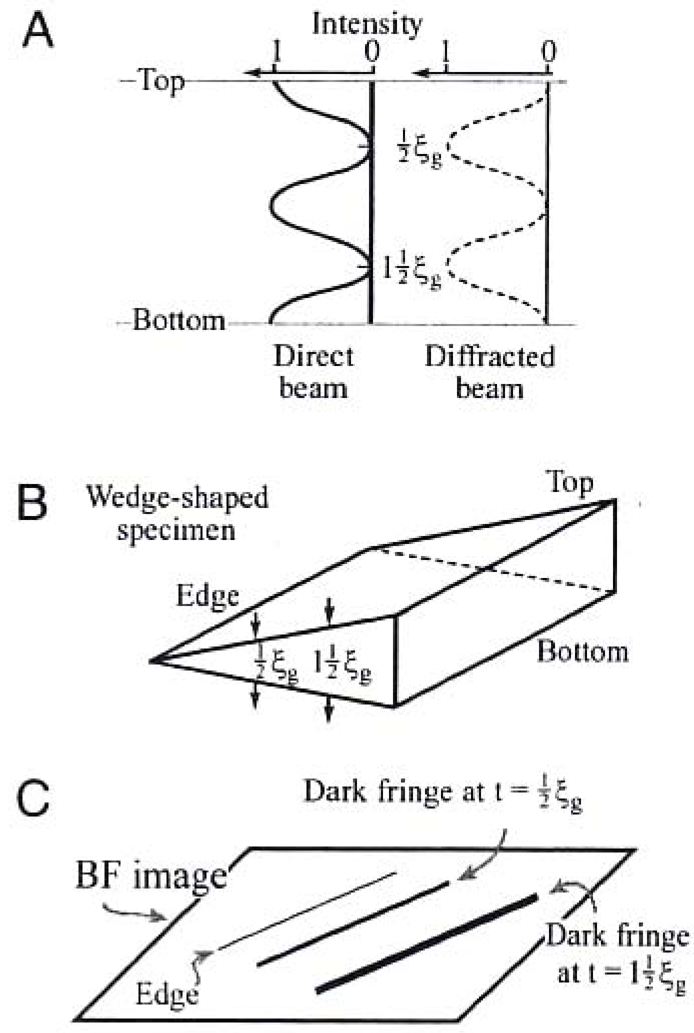


**Figure 23.2.** (A) At the Bragg condition ($s = 0$), the intensities of the direct and diffracted beams oscillate in a complementary way. (B) For a wedge specimen, the separation of the fringes in the image (C) is determined by the angle of the wedge and the extinction distance, $\xi_g$.

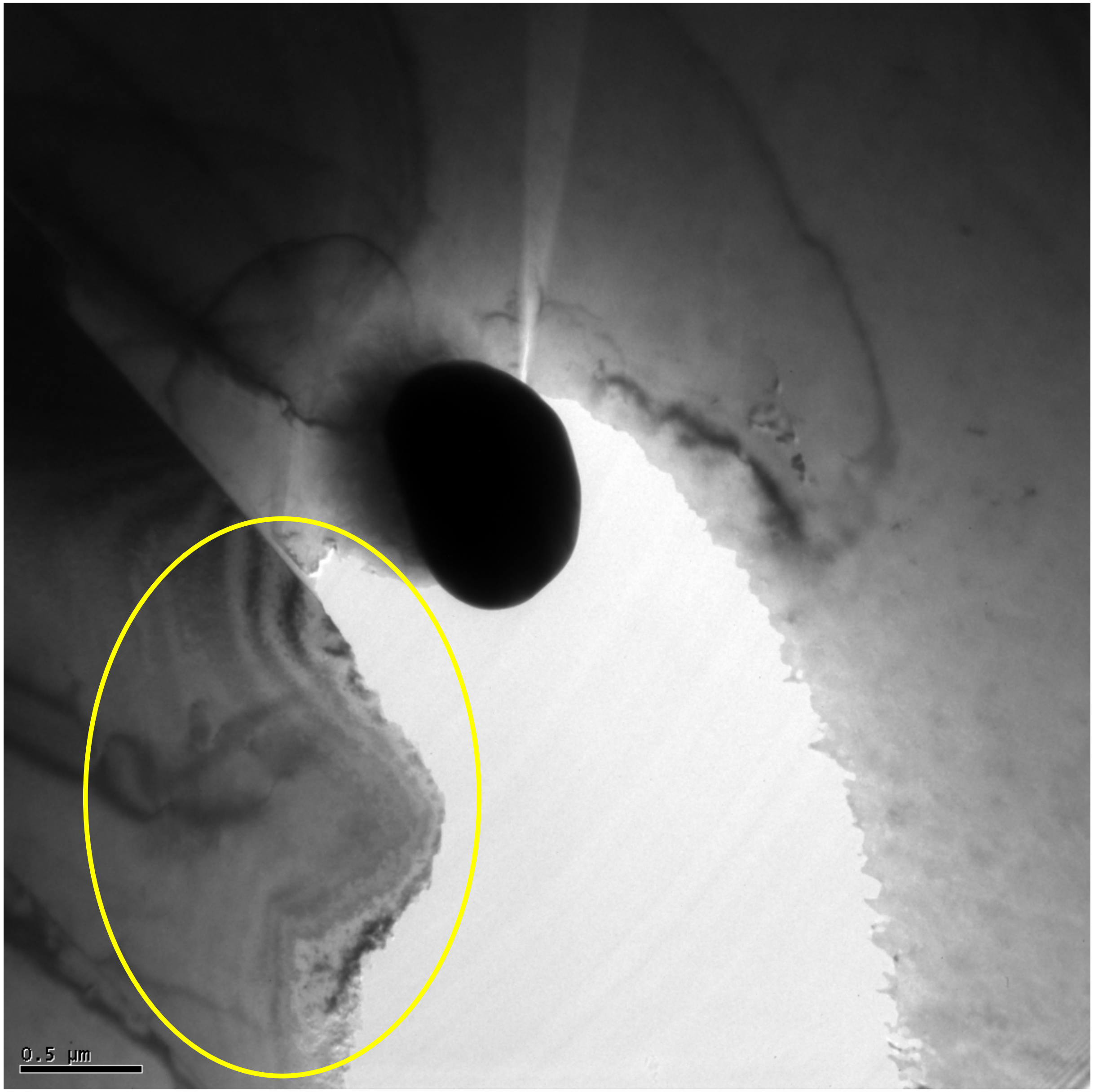


Líneas de espesor en Cu-Co-Ti

# Defectos planares

- Fallas de apilamiento
- Bordes de grano
- APB (Anti-phase boundaries)

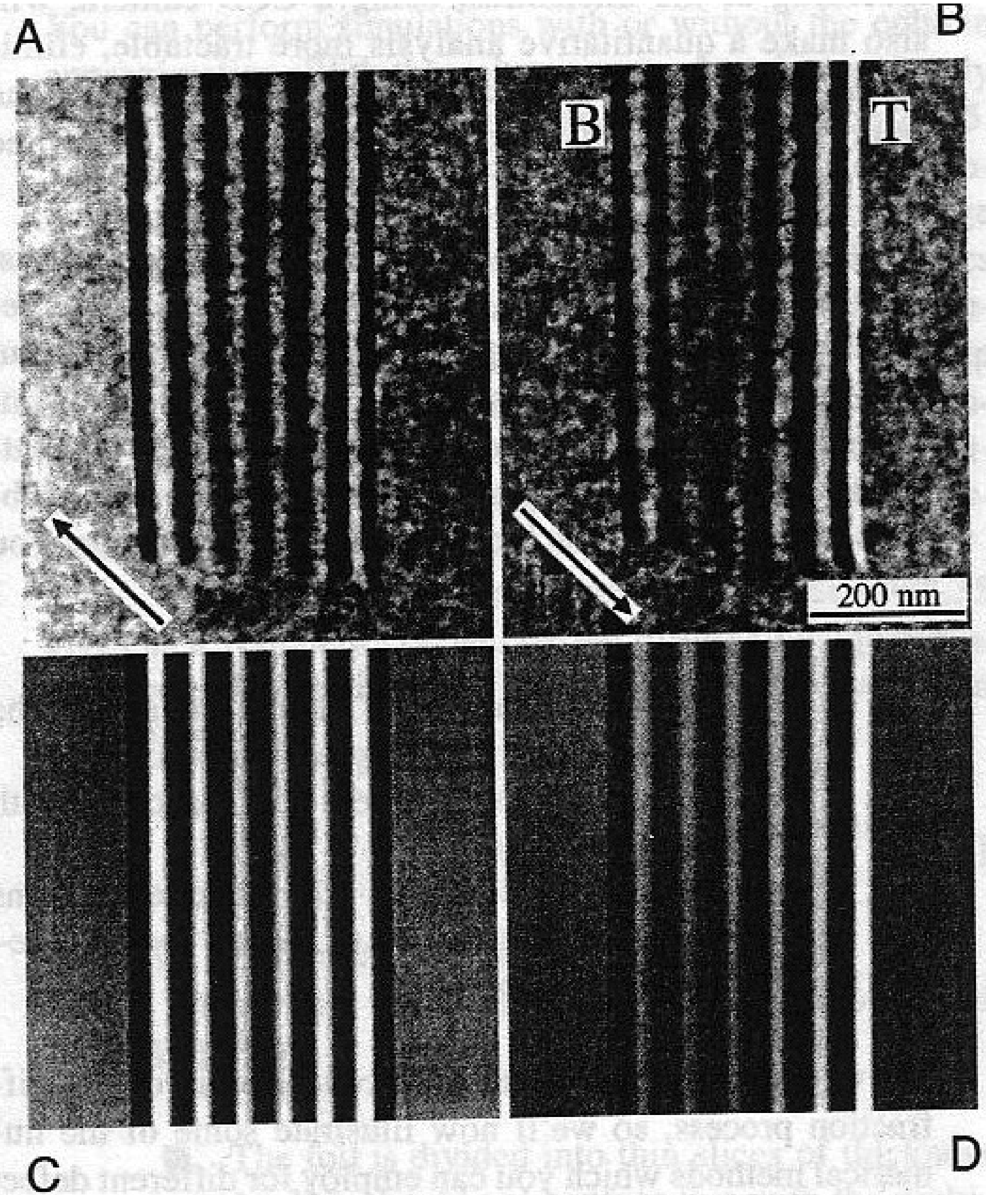


**Figure 24.16.** (A) Experimental BF image of an APB with $\mathbf{g} = 220$. (B) DF image of the same defect, $\mathbf{g} = \bar{2}20$. (C,D) Corresponding simulated images.

# Campos de deformación

- Dislocaciones
- Partículas

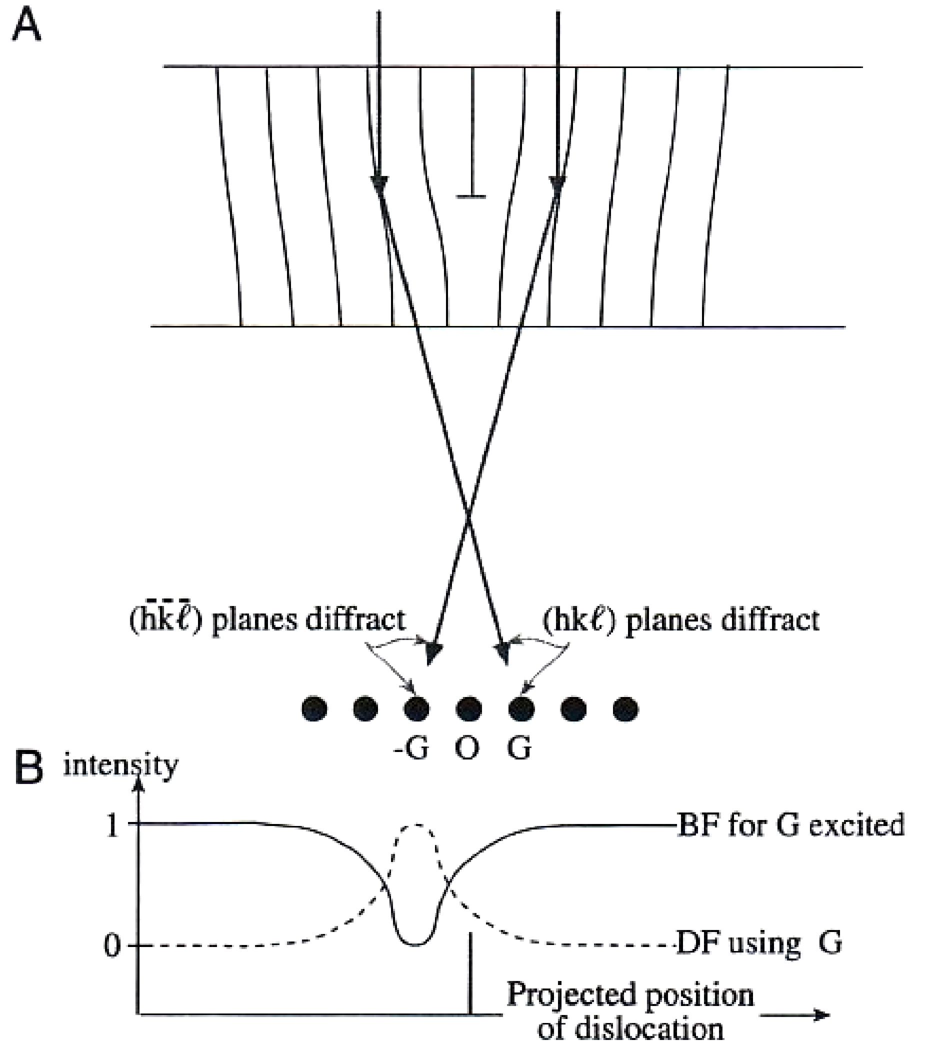


**Figure 25.1.** (A) The specimen is tilted slightly away from the Bragg condition ($\mathbf{s} \neq 0$). The distorted planes close to the edge dislocation are bent back into the Bragg-diffracting condition ($\mathbf{s} = 0$), diffracting into G and –G as shown. (B) Schematic profiles across the dislocation image showing that the defect contrast is displaced from the projected position of the defect.

# Ejemplos dislocaciones

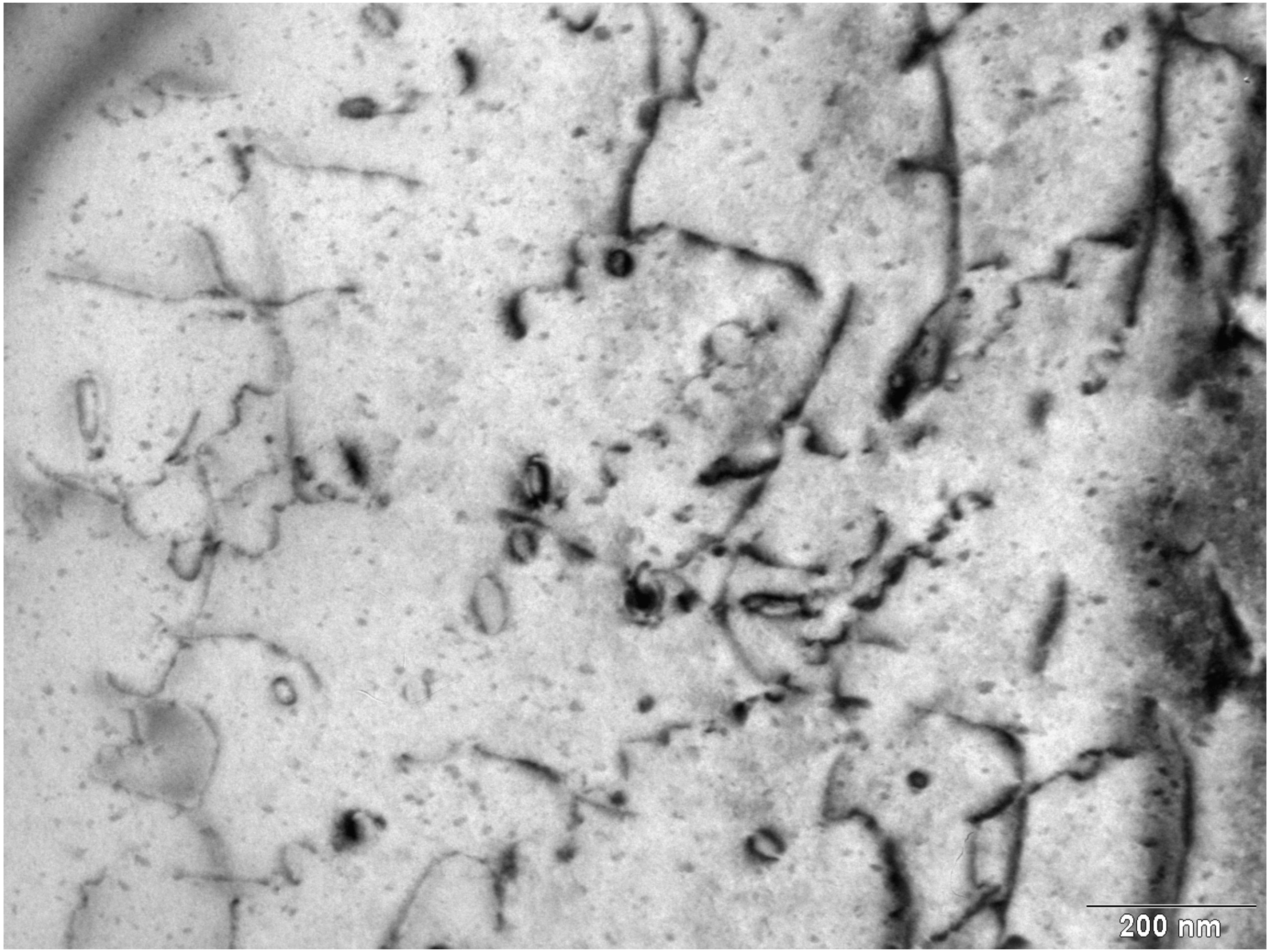


Loops de dislocaciones en Al-Cu-Mg-Fe-Ni-Sc

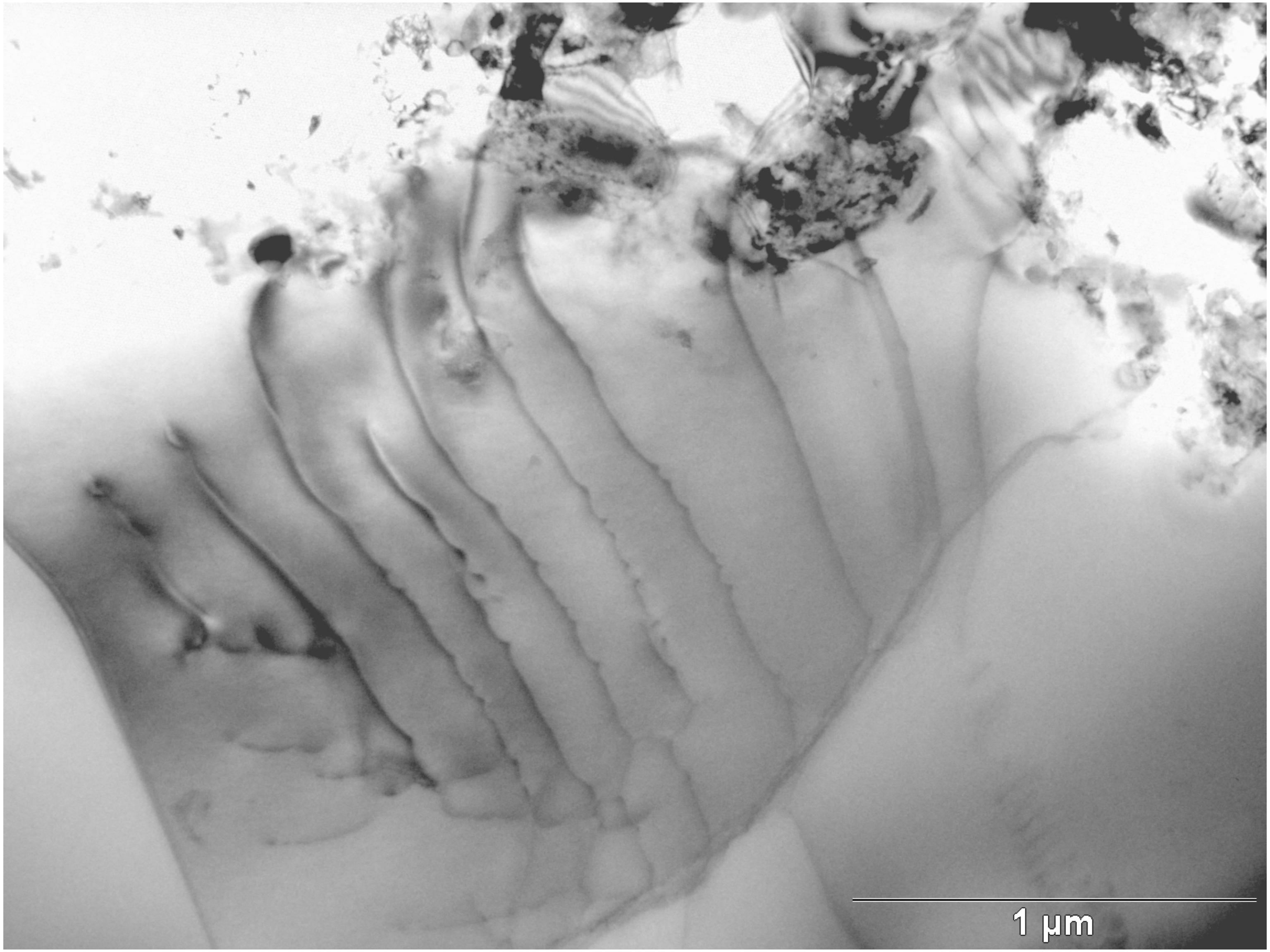


Estructura de dislocaciones en Al-Cu-Mg-Fe-Ni-Sc

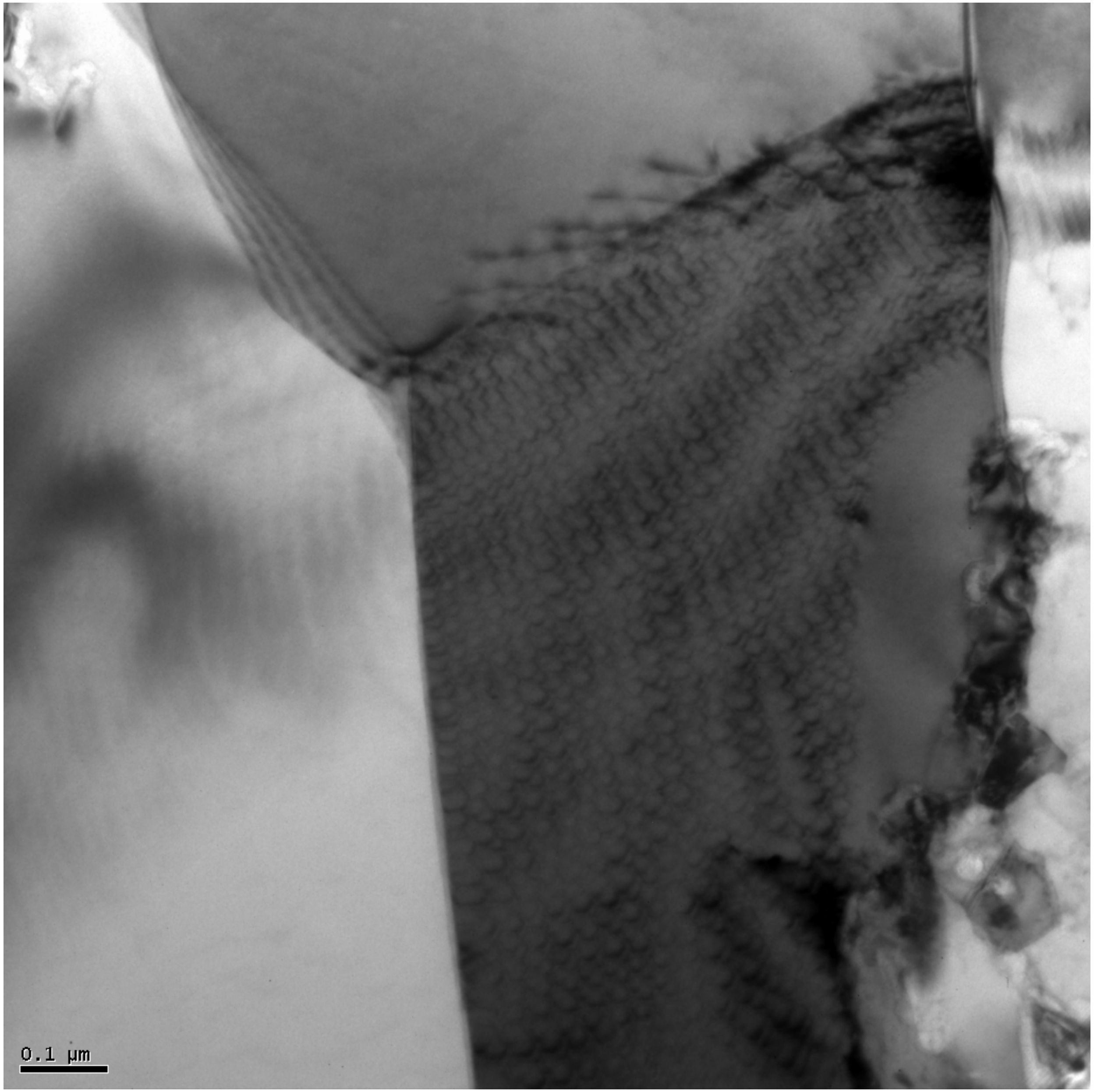


Estructura de dislocaciones en Al-Mg

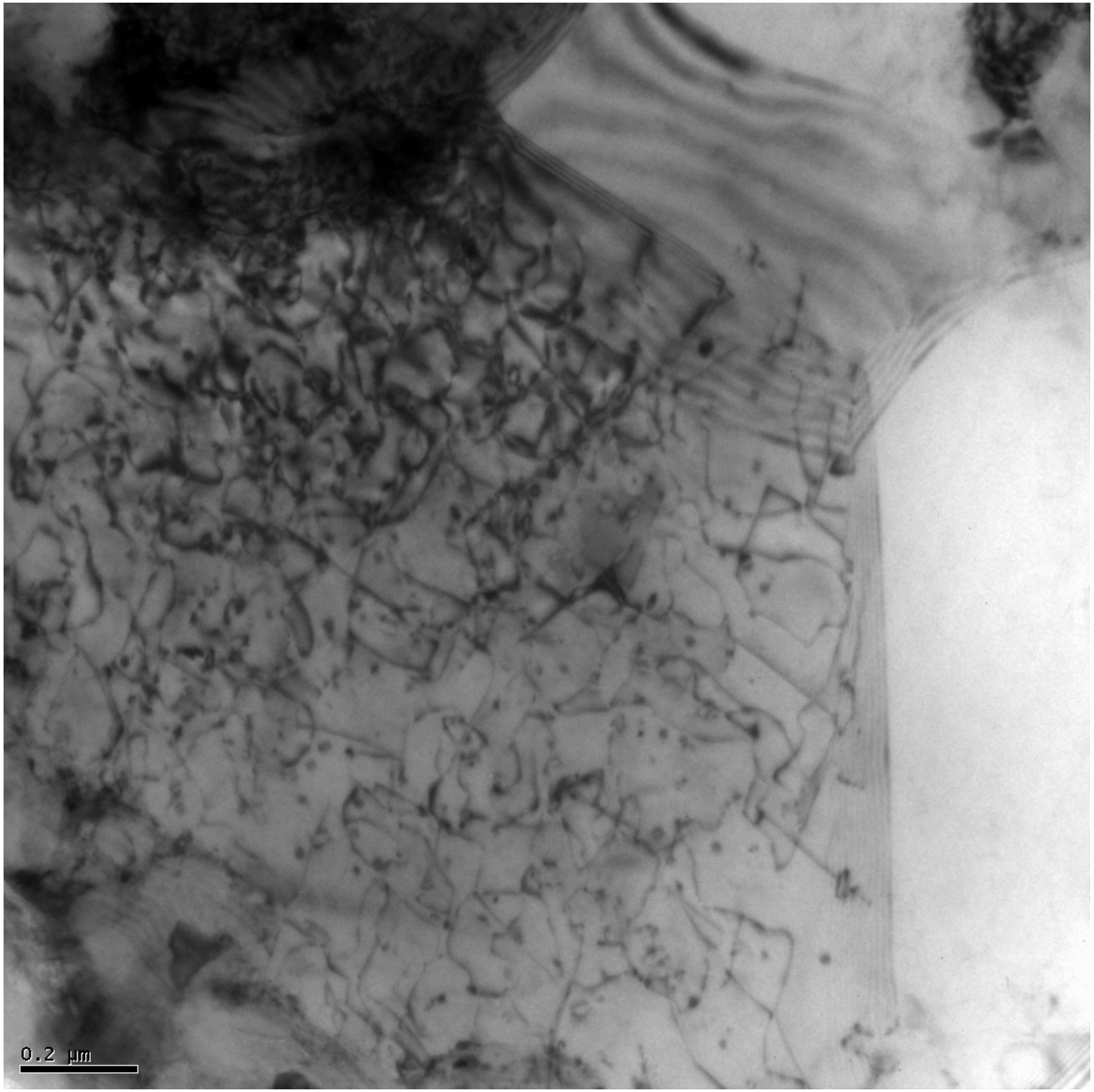


Al-Mg deformado

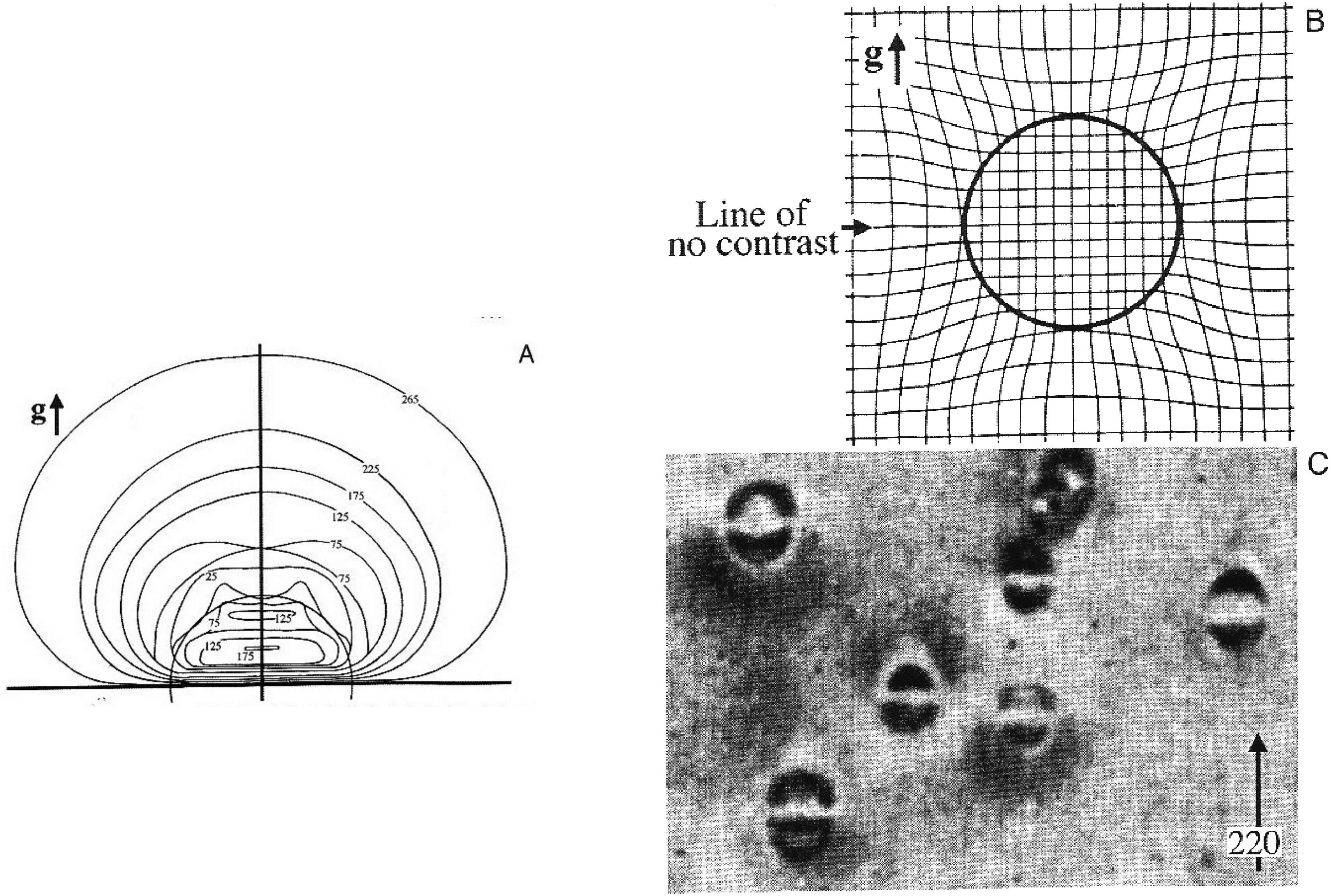


**Figure 25.26.** (A) Intensity contours from a simulated image of a particle like that shown schematically in (B). Notice the line of no contrast which corresponds to the plane that is not distorted by the strain field of the particle. (C) Experimental image of coherent particles in Cu-Co showing strain contrast.

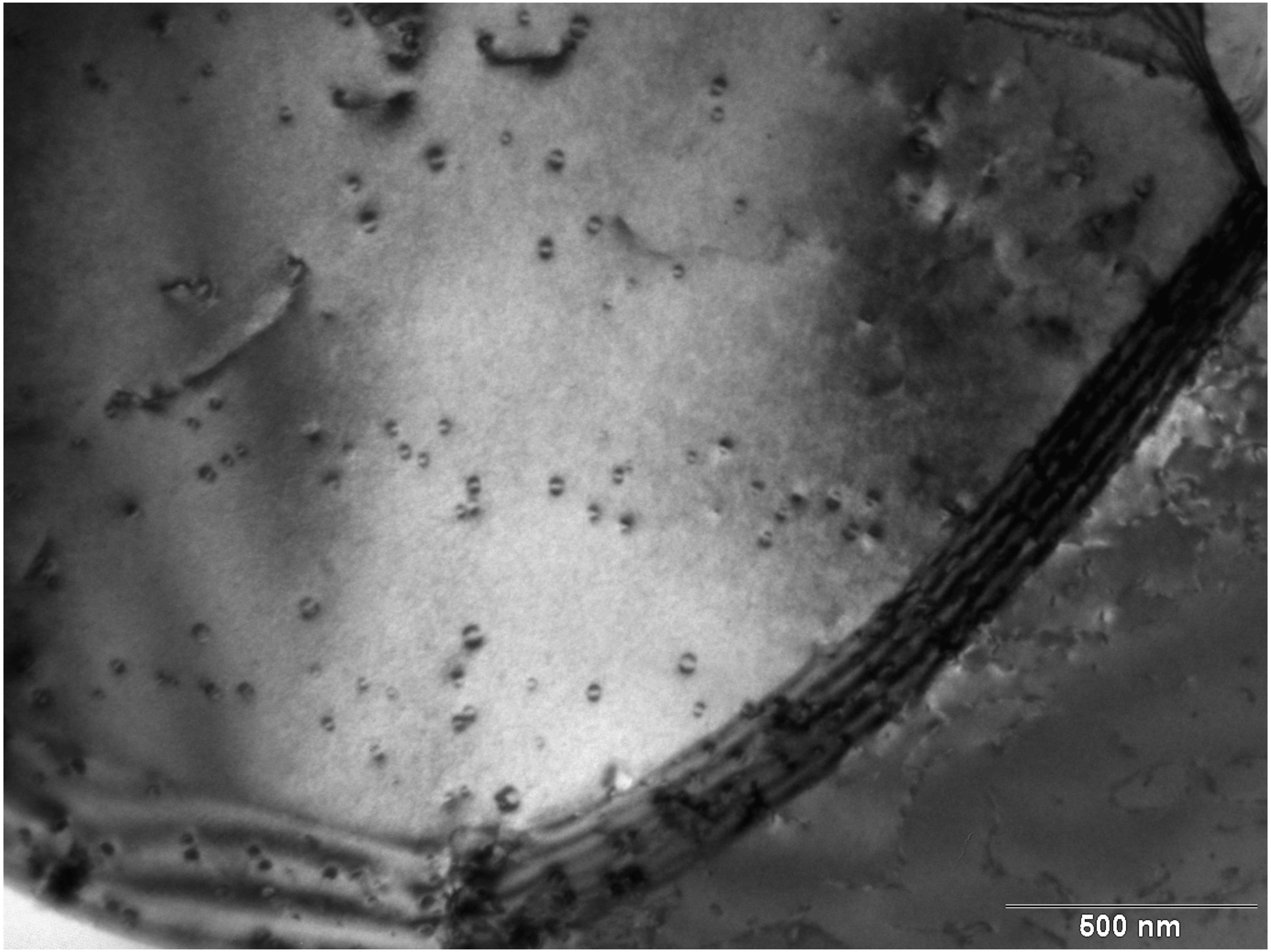


Partículas coherentes de $Al_3Sc$ en Aluminio

# Contraste por fase

$$\Psi = \phi_{\mathbf{0}}(z)e^{2\pi i \mathbf{k}_{\mathrm{I}}\cdot\mathbf{r}} + \phi_{\mathbf{g}_1}(z)e^{2\pi i \mathbf{k}_{\mathrm{D}1}\cdot\mathbf{r}} + \phi_{\mathbf{g}_2}(z)e^{2\pi i \mathbf{k}_{\mathrm{D}2}\cdot\mathbf{r}} + \cdots$$

A

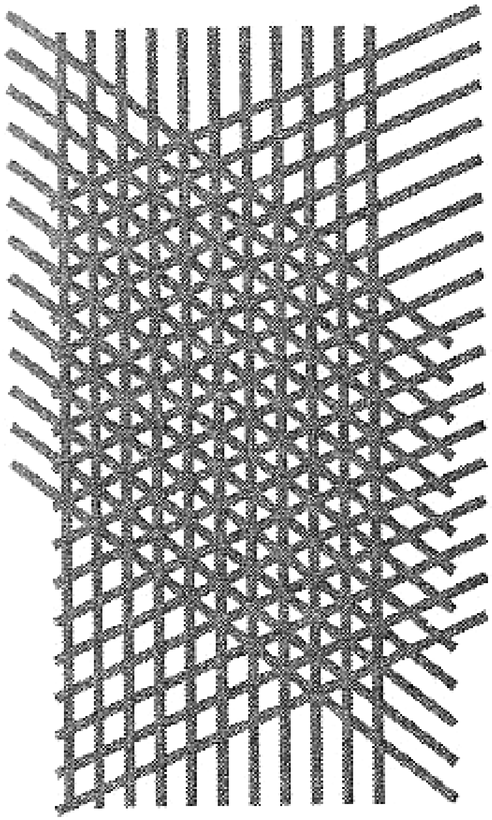

B

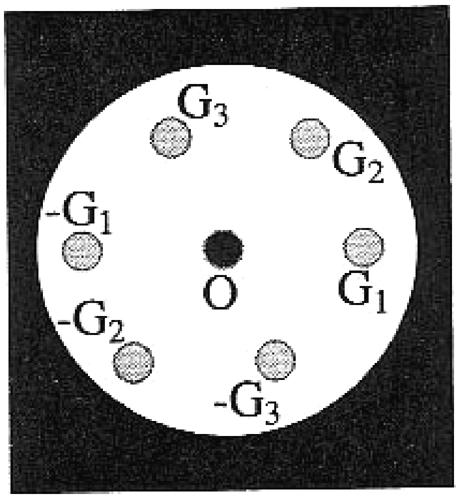


**Figure 27.2.** (A) Schematic many-beam image showing crossing lattice fringes and (B) the diffraction pattern.

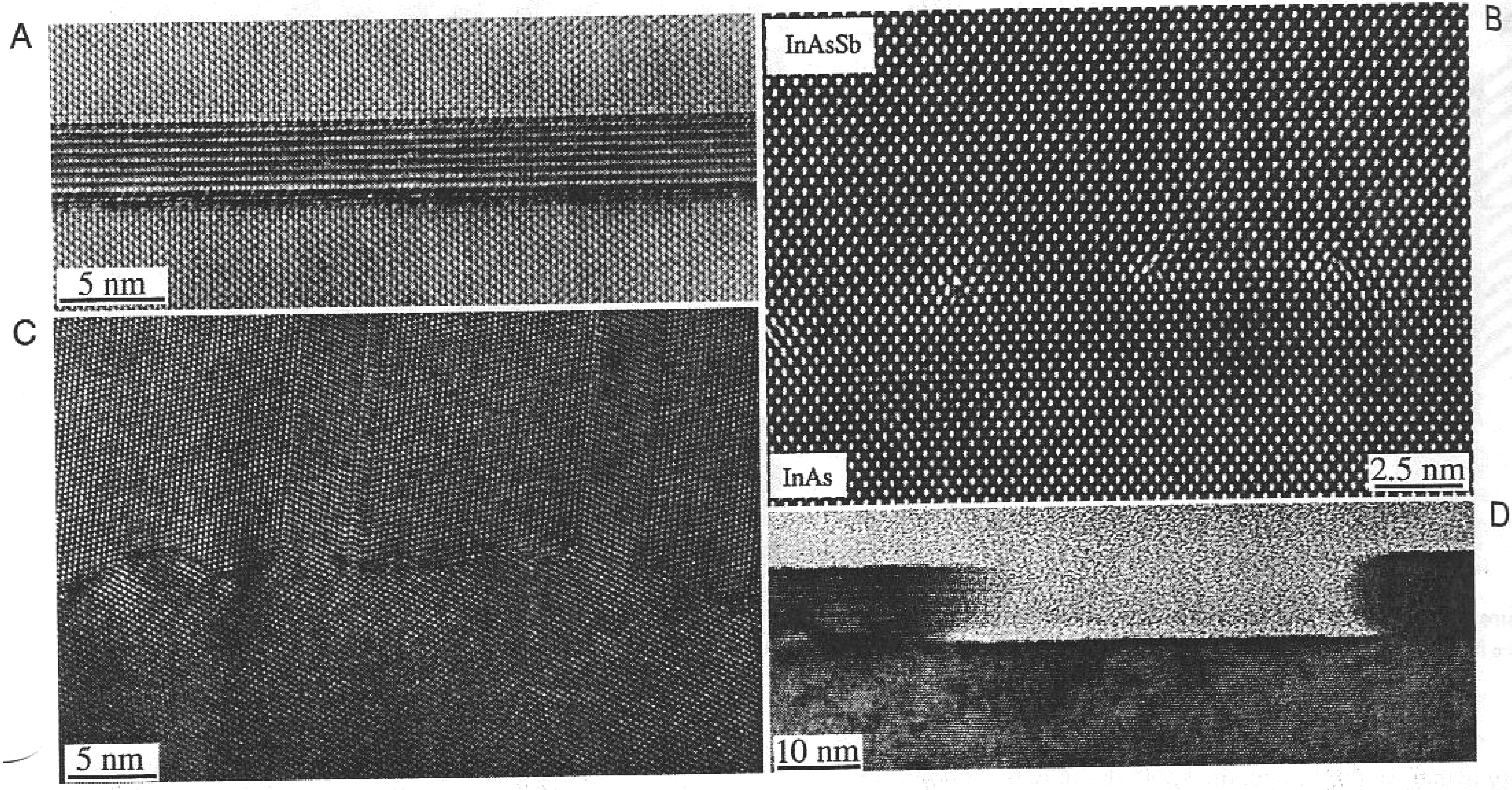


**Figure 27.4.** Illustrations of lattice images which contain easily interpreted information. (A) The spinel/olivine interface; (B) dislocations at a heterojunction between InAsSb and InAs; (C) a grain boundary in Ge faceting on an atomic scale; (D) a profile view of a faceted surface.

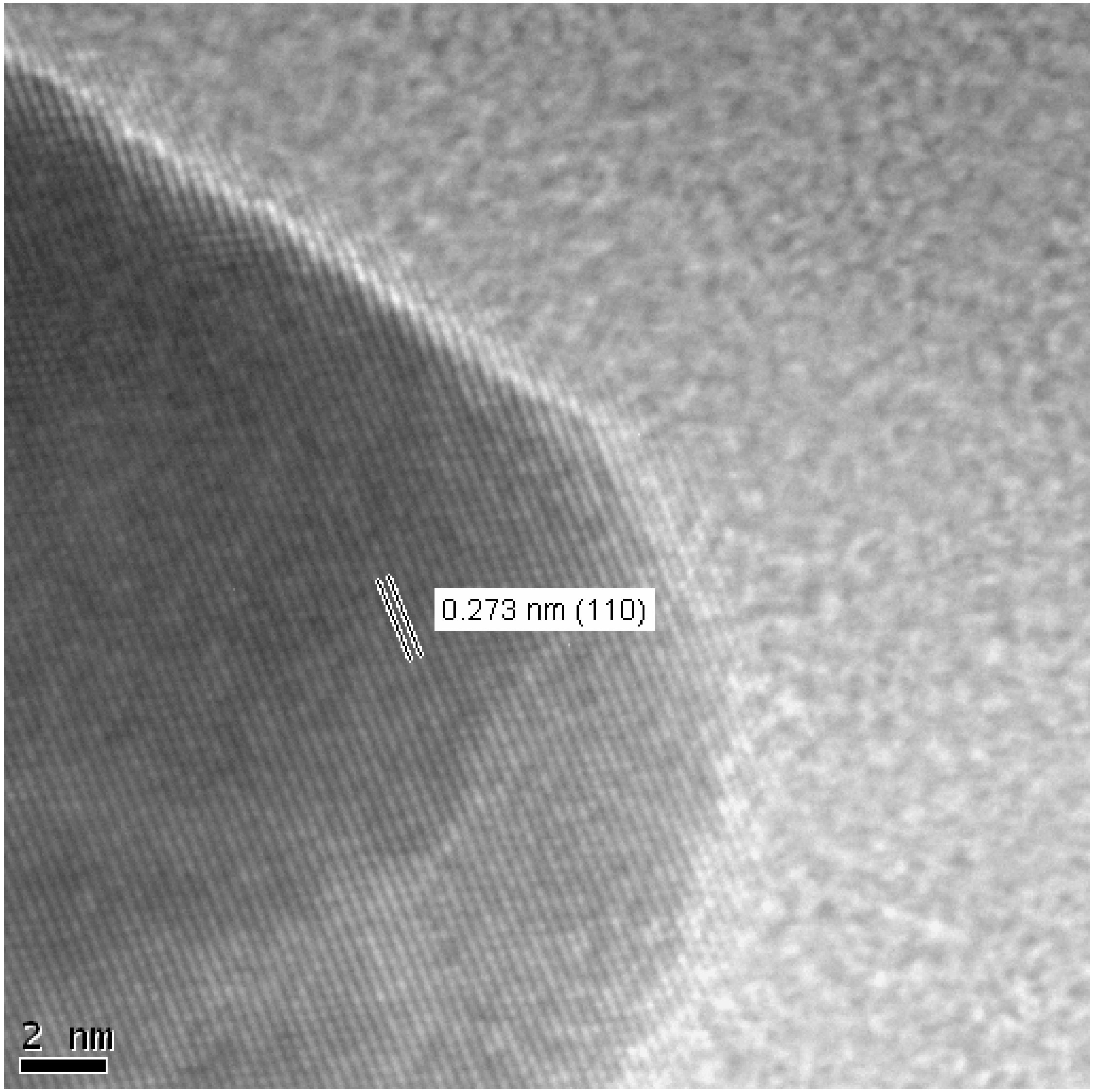


**Nanoplacas de CuO**

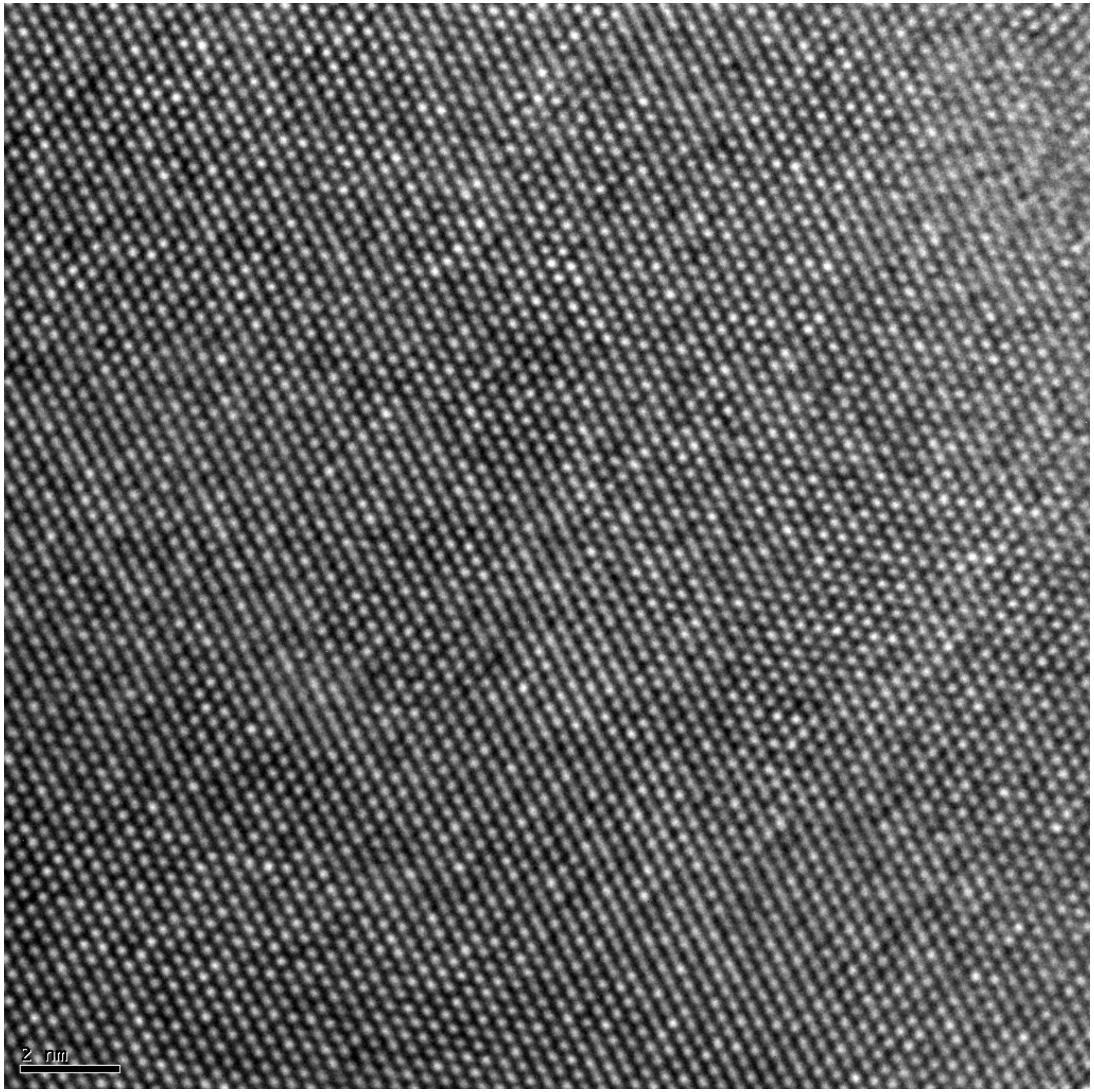


**Si monocristalino**

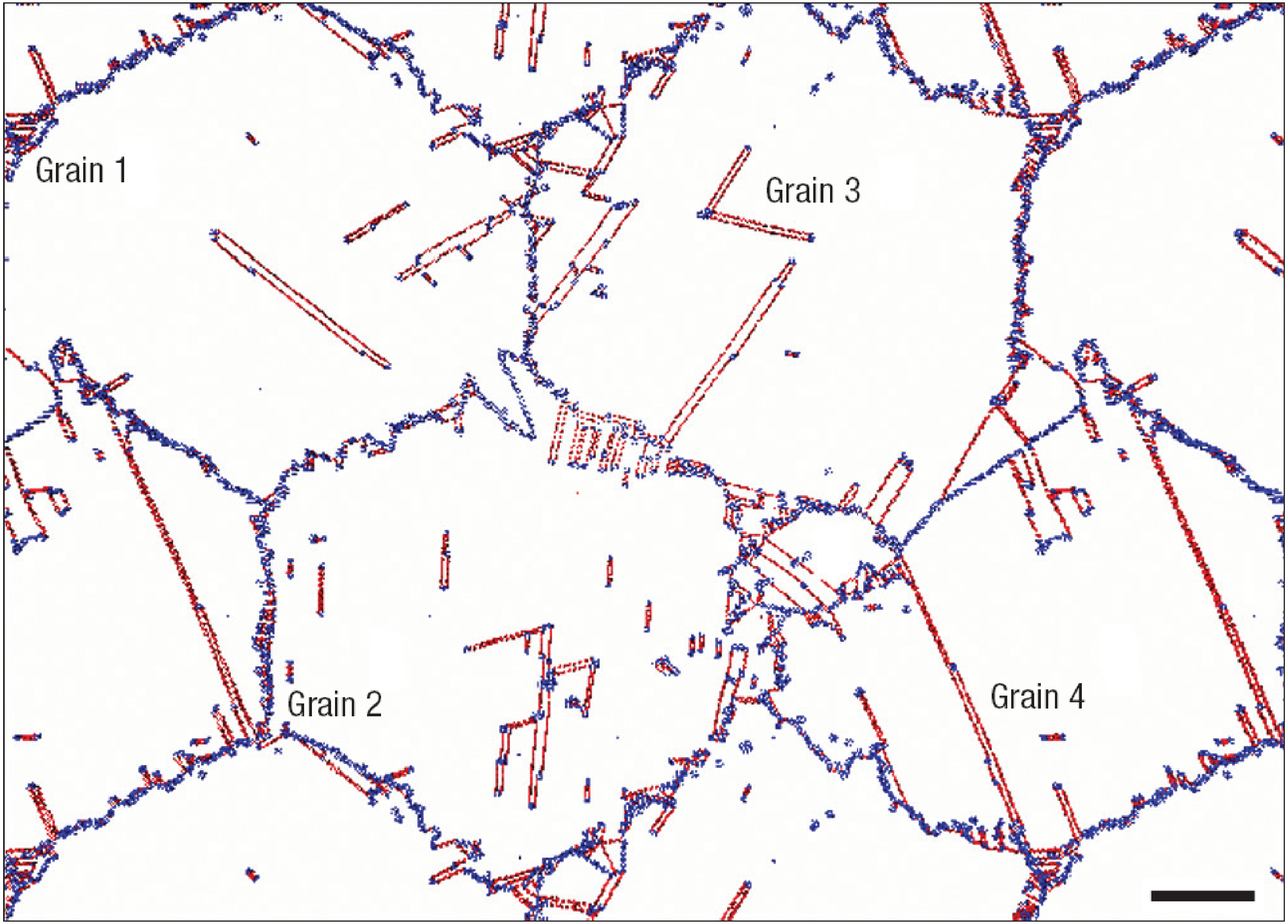


V. Yamakov et al., *Acta Materialia,* 51 (2003), pp. 4135-4147

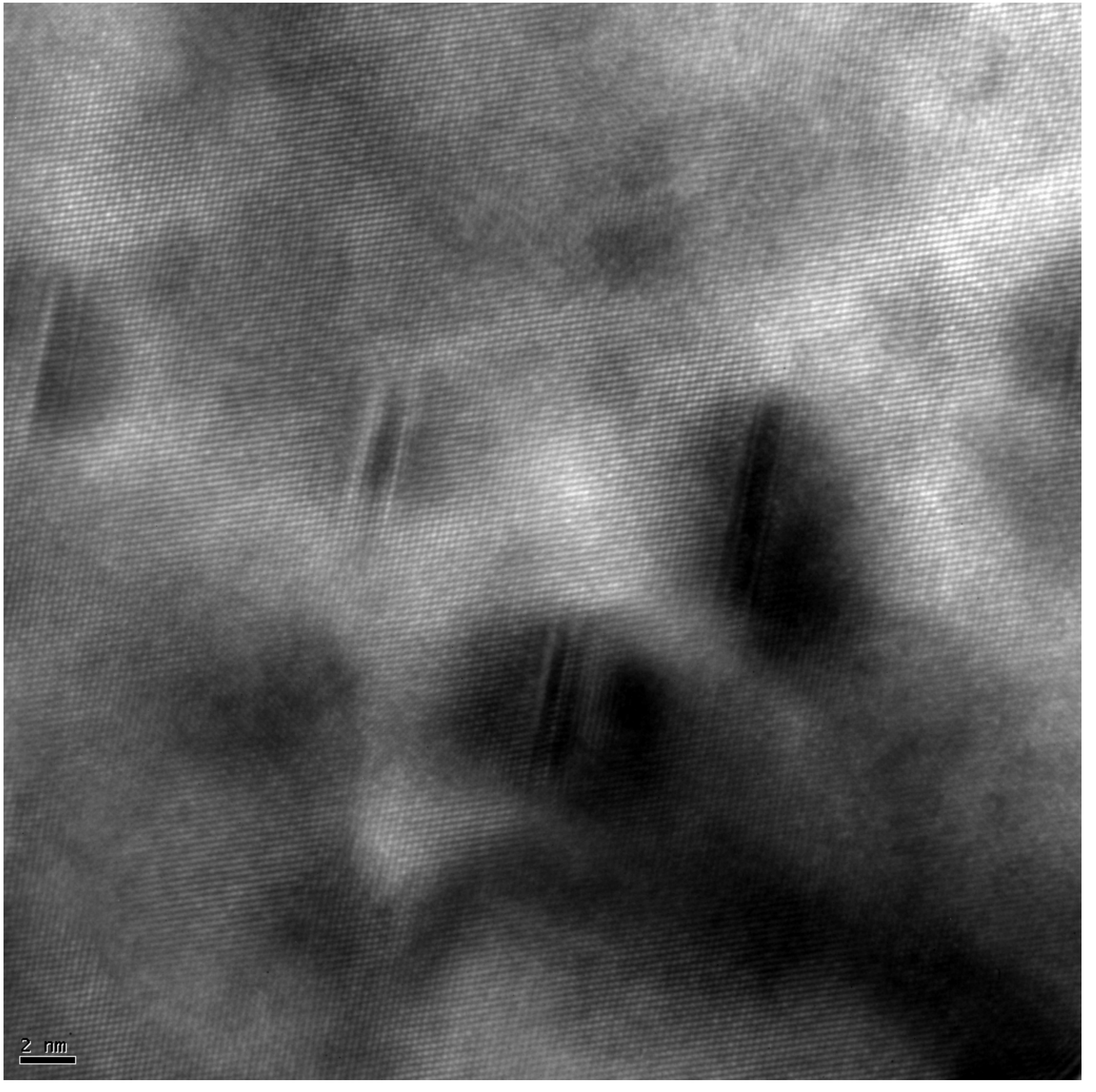


Nano-twins en Al-Cu-Mg-Fe-Ni-Sc

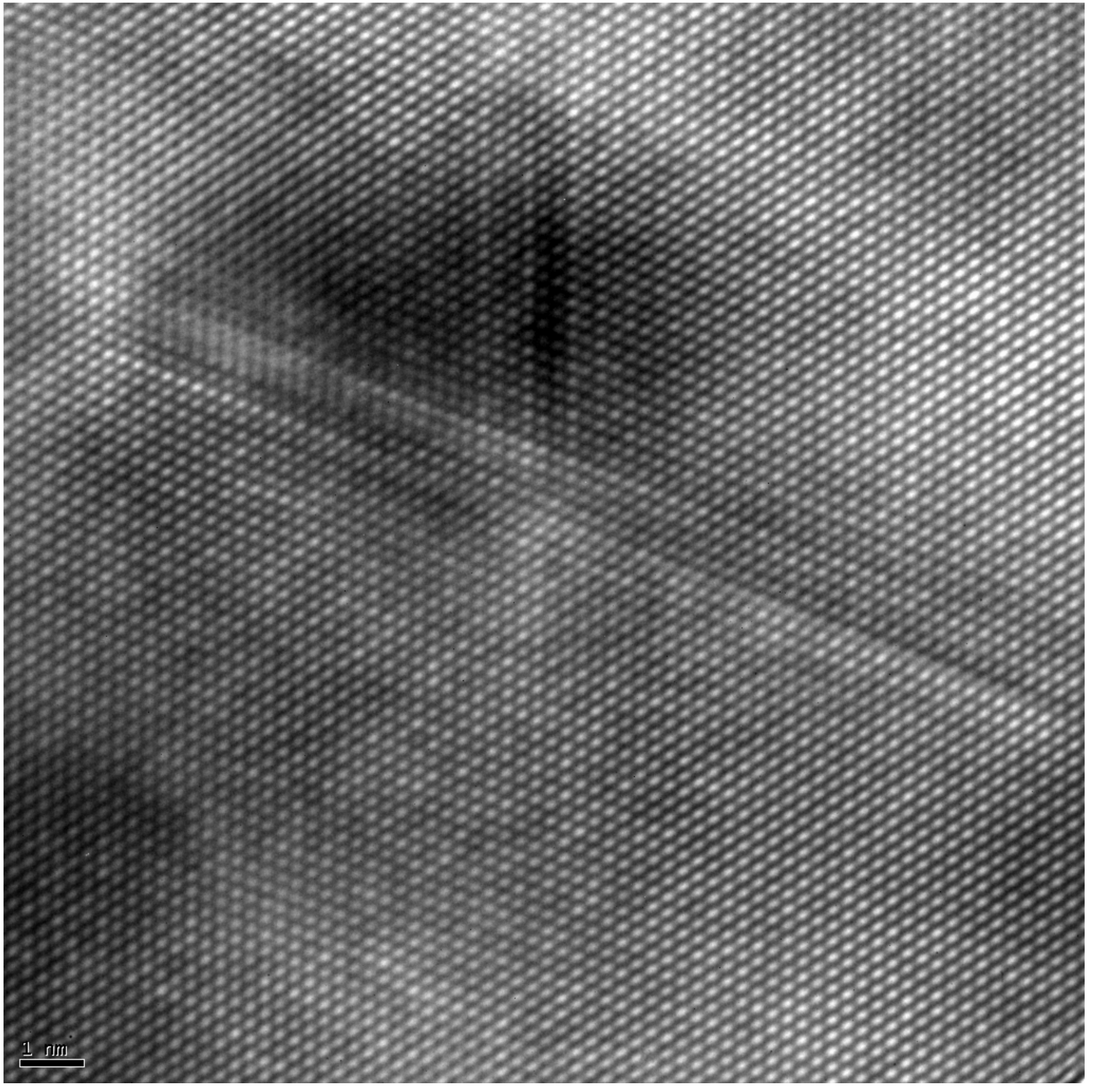


Nano-twins en Al-Cu-Mg-Fe-Ni-Sc

# STEM

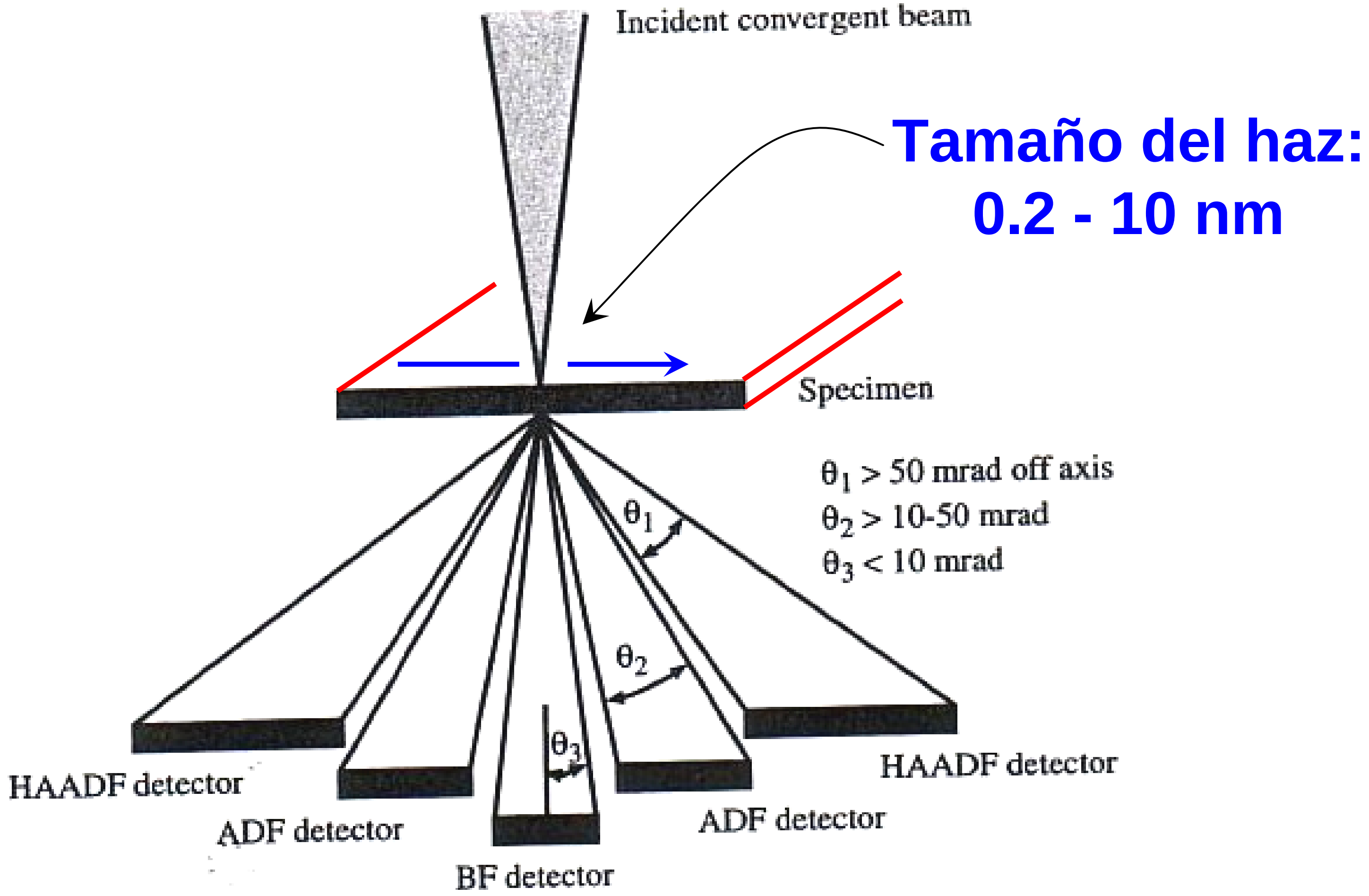


- Modo de imagen que involucra un haz convergente y de pequeño tamaño
- Barrido, similar al SEM
- Produce imágenes de campo claro, oscuro, y de contraste Z (HAADF)
- Sirve para producir mapas y perfiles de composición química (EDS o EELS), y mapas de orientación cristalográfica (CBED)

# Contraste Z

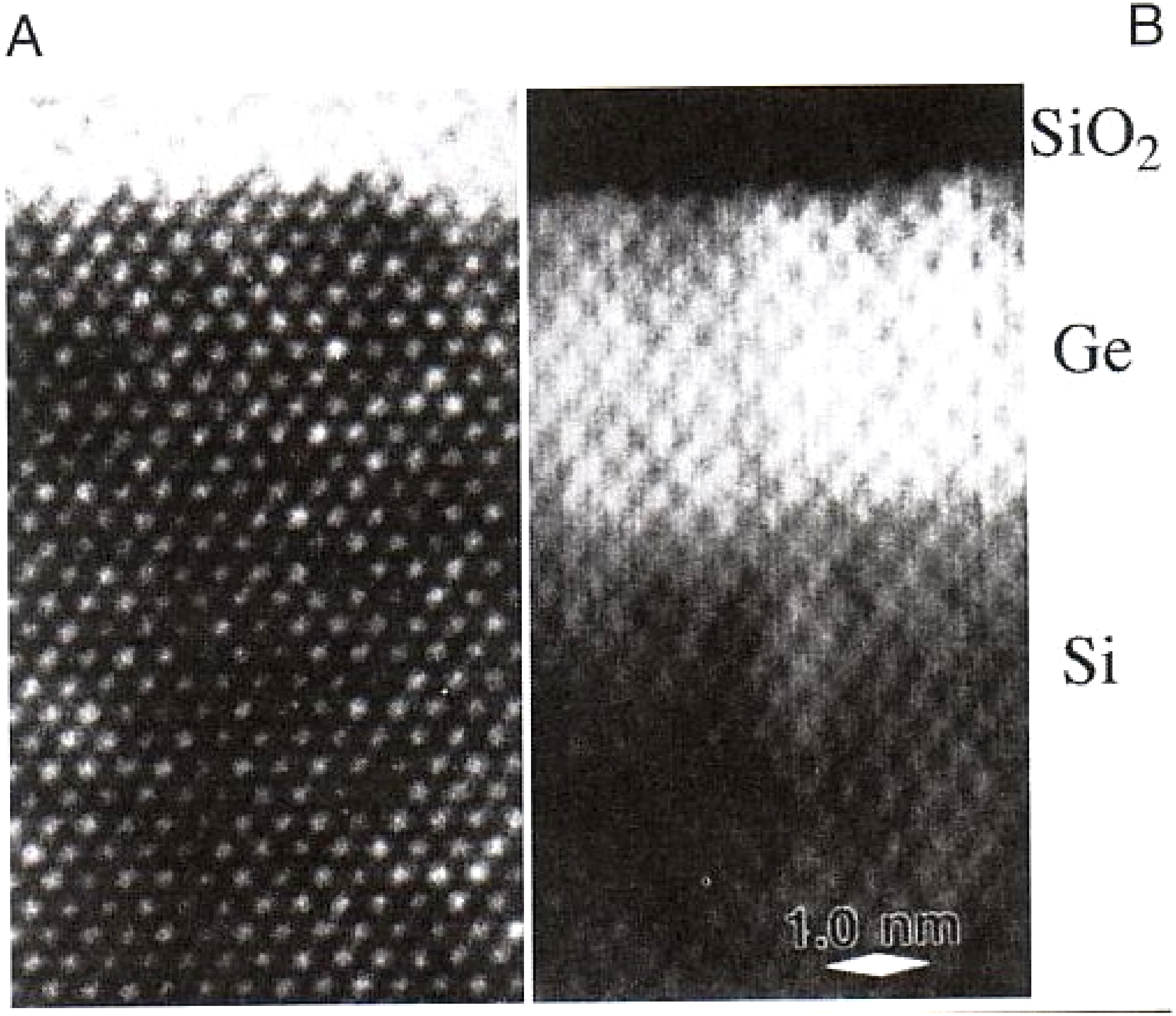


HRTEM Contraste Z (HAADF)